

VALIDATED SEISMIC DESIGN GUIDELINES FOR SOLID AND PERFORATED HYBRID PRECAST SHEAR WALLS

Brian J. Smith, MS, PE, Dept. of Civil Eng. and Geo. Sci., Univ. of Notre Dame, USA
Yahya C. Kurama, PhD, PE, Dept. of Civil Eng. and Geo. Sci., Univ. of Notre Dame, USA

ABSTRACT

This paper provides validated seismic design guidelines for special unbonded post-tensioned “hybrid” precast concrete shear walls. These walls utilize a combination of mild steel [Grade 400 (U.S. Grade 60) steel] and high-strength unbonded post-tensioning (PT) steel for lateral resistance across horizontal joints, resulting in an efficient structure. The mild steel reinforcement is designed to yield in tension and compression, providing energy dissipation. The unbonded PT steel provides self-centering capability to reduce the residual lateral displacements of the structure after a large earthquake. The paper summarizes key aspects of the recommended seismic design and detailing of the walls, with supporting experimental evidence from six 0.4-scale wall test specimens. The design guidelines are aimed to allow practicing engineers and precast concrete producers to design American Concrete Institute compliant special hybrid shear walls with predictable and reliable seismic behavior. Ultimately, the results from this project support the U.S. code approval of the hybrid precast wall system for moderate and high seismic regions, while also presenting important design, detailing, and analysis considerations to prevent undesirable failure mechanisms.

Keywords: Horizontal Joints, Hybrid Shear Walls, Perforated Shear Walls, Precast Concrete, Seismic Design, Seismic Testing

INTRODUCTION AND BACKGROUND

As described in Smith and Kurama¹ and Smith et al.,²⁻⁴ the hybrid precast wall system investigated in this research (Fig. 1) utilizes a combination of mild steel bars [i.e., Grade 400 (U.S. Grade 60) steel bars] and high-strength unbonded post-tensioning (PT) strands for lateral resistance across horizontal joints. Under the application of lateral loads into the nonlinear range, the primary mode of displacement in these walls occurs through gap opening at the horizontal joint between the base panel and the foundation, allowing the wall to undergo large lateral displacements with little damage. Upon unloading, the PT steel provides a restoring force to close this gap, thus reducing the residual lateral displacements of the wall after a large earthquake. The use of unbonded tendons delays the yielding of the PT strands and reduces the tensile stresses transferred to the concrete (thus reducing cracking) as the tendons elongate under lateral loading. The mild steel bars across the base joint are designed to yield in tension and compression, providing energy dissipation through the gap opening/closing behavior under reversed-cyclic lateral loading. A pre-determined length of these energy dissipating (E.D.) bars is unbonded at the bottom of the wall (by wrapping the bars with plastic sleeves) to reduce the steel strains and prevent low-cycle fatigue fracture.

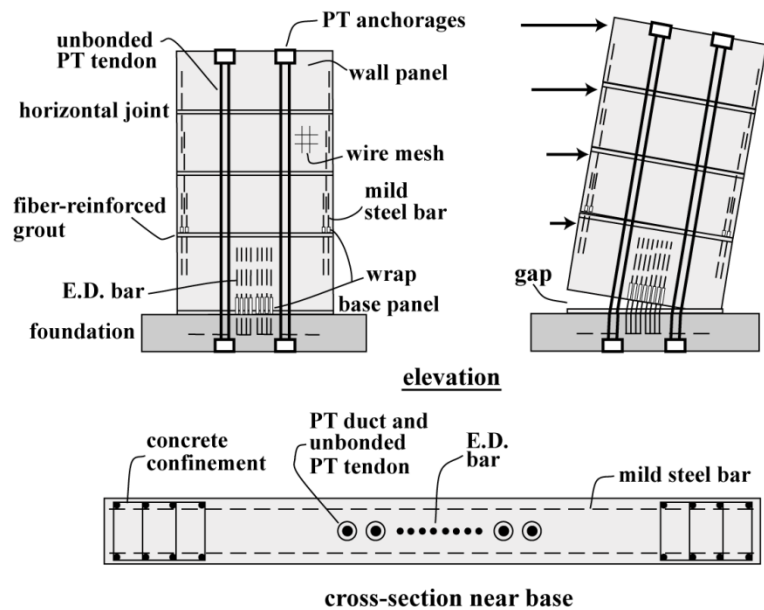


Fig. 1 Elevation, Exaggerated Displaced Position, and Cross Section of Hybrid Wall

The hybrid precast wall system offers high quality production, relatively simple construction, and excellent seismic characteristics by providing self-centering to the building as well as energy dissipation to control the lateral displacements. Despite these desirable characteristics, hybrid precast walls are classified as “non-emulative” structures since their behavior is different than the behavior of conventional cast-in-place reinforced concrete shear walls. Thus, experimental validation is required by ACI 318-11⁵ and ACI ITG-5.1⁶ prior to the use of these structures in seismic regions of the U.S.

RESEARCH OBJECTIVE

The primary objective of this research project is to support the validation of hybrid precast wall structures with practical construction details as “special” reinforced concrete shear walls

through an integrated experimental and analytical study. The project provides new information in accordance with and directly addressing the ACI ITG-5.1 validation requirements as well as information regarding the behavior of hybrid precast walls featuring multiple wall panels (i.e., multiple horizontal joints) and panel perforations, both common features in practical building construction. The experimental results demonstrate that properly designed and detailed hybrid walls can satisfy all requirements for special reinforced concrete shear walls in high seismic regions with improved performance.

DESIGN PROCEDURE DOCUMENT

A key deliverable from this research project is a Design Procedure Document¹ containing specific design, detailing, and analysis guidelines, including appropriate capacity reduction factors, for the application of hybrid precast walls as special reinforced concrete shear walls in moderate and high seismic regions of the U.S. Both a performance-based design procedure and a prescriptive procedure are provided. This paper summarizes key recommendations from the performance-based design procedure. Where appropriate, ACI 318-11 requirements for conventional monolithic cast-in-place reinforced concrete structures are utilized to help in the adoption of the hybrid wall design guidelines by practicing engineers. Furthermore, applicable references and suggested revisions to the design recommendations in ACI ITG-5.2⁷ are included. A detailed example demonstrating a step-by-step application of the design can be found in the Design Procedure Document.

The Design Procedure Document¹ can be used to design hybrid walls with height-to-length (H_w/L_w) aspect ratios equal to or greater than 0.5 in low to mid-rise structures with a practical height limitation of 36.5-m (120-ft) or approximately eight to ten stories tall. The procedure is applicable to both single-panel wall systems (featuring only the base-panel-to-foundation joint) as well as multi-panel systems (featuring the base-panel-to-foundation joint as well as upper panel-to-panel joints) with or without panel perforations. The guidelines were validated using the measured and predicted behaviors of six 0.4-scale wall test specimens (four solid and two perforated walls) subjected to service-level gravity loads combined with quasi-static reversed-cyclic lateral loading.² Table 1 provides some of the important features of these wall specimens. For the tested wall dimensions of $H_w=5.49$ -m (18-ft) and $L_w=2.44$ -m (8-ft), the prescribed “validation-level” wall drift per ACI ITG-5.1 for each specimen was $\Delta_w=2.30\%$, where the wall drift, Δ_w is defined as the lateral displacement at the top of the wall divided by the wall height, H_w .

While outside the scope of this paper, the Design Procedure Document¹ includes analysis tools such as a linear-elastic effective stiffness model and a basic finite element model for nonlinear monotonic pushover analysis (the finite element model is an aid to design hybrid walls with perforations). The analytical modeling recommendations intentionally incorporate several simplifying assumptions appropriate for the design office. The Design Procedure Document also presents a detailed fiber element model that can be used to conduct reversed-

cyclic and dynamic analyses of hybrid walls; however, this model is not a necessary tool for seismic design.

Table 1 Selected Specimen Properties

Spec. No.	Panel Perf. (cm)	κ_d		PT Tendons			E.D. Bars					Confined Region		
		Design	Actual	No. of strands and diameter	f_p/f_{pu}	Eccentricity e_p (cm)	Size	Eccentricity e_s (cm)	Wrapped Length (cm)	$\epsilon_{sm}/\epsilon_{su}$	Continuity at Base	l_h (cm)	s_h (cm)	s_{bot} (cm)
HW1	-	0.50	0.53	3 – 1.27-cm	0.54	±23	No. 19	±7.5, 15	25	0.64	Spliced	40	8.3	5.0
HW2	-	0.50	0.53	3 – 1.27-cm	0.54	±23	No. 19	±7.5, 15	25	0.61	Spliced	40	8.3	1.9
HW3	-	0.50	0.50	3 – 1.27-cm	0.54	±28	No. 19	±8.9, 19	38	0.48	Cont.	40	7.6	1.9
HW4	36x51	0.50	0.54	3 – 1.27-cm	0.54	±28	No. 19	±8.9, 19	38	0.49	Cont.	47	6.4	1.9
HW5	43x51	0.85	0.90	2 – 1.27-cm	0.54	±14	No. 22	±23, 86	25, 40	0.85	Cont.	47	6.4	1.9
EW	-	-	-	-	-	-	No. 22	±79, 91, 104	56	0.73	Spliced	20	8.3	1.9

f_p =average initial strand stress; f_{pu} =design ultimate strength of strand [1862-MPa (270-ksi)]; ²measured from wall centerline; ϵ_{sm} =maximum expected (design) E.D. bar strain at $\Delta_w=2.30\%$; ϵ_{su} =strain at maximum (peak) strength of E.D. steel from monotonic material testing; ⁴confined region length at wall toes (center-to-center of bar); ⁵confinement hoop spacing (center-to-center of bar); ⁶first hoop distance from bottom of base panel (to center of bar)

DETERMINATION OF SEISMIC FORCES AND DRIFT DEMANDS

The design of a hybrid wall should be conducted under all applicable load combinations prescribed by ASCE-7,⁸ including the use of a redundancy factor and torsional effects from accidental and applied eccentricities. The design base shear force can be obtained using any of the procedures allowed in ASCE-7, such as the equivalent lateral force procedure or modal analysis procedure. When selecting the response modification factor, R using Table 12.2-1 in ASCE-7, the seismic force-resisting system for hybrid walls can be classified as “special reinforced concrete shear walls.” Therefore, the response modification factors should be taken as $R=5.0$ and 6.0 for bearing wall systems and building frame systems, respectively.

The design is conducted at two drift levels: (1) the design-level wall drift, Δ_{wd} corresponding to the design basis earthquake (DBE); and (2) the maximum-level wall drift, Δ_{wm} corresponding to the maximum considered earthquake (MCE). Appropriate analytical techniques, such as nonlinear dynamic response history analyses under properly selected DBE and MCE ground motion sets can be used to determine these drifts. Alternatively, the ASCE-7 guidelines in Section 12.8.6 can be used to determine the design-level wall drift, while the maximum-level wall drift can be calculated as:

$$\Delta_{wm} = 0.95\Delta_{wc} \quad (1)$$

with

$$\Delta_{wc} = 0.9\% \leq \left(\frac{H_w}{L_w}\right) 0.8\% + 0.5\% \leq 3.0\% \quad (2)$$

where, Eqn. 2 is adopted from ACI ITG-5.1 as the minimum drift capacity of special unbonded post-tensioned precast concrete shear walls.

DESIGN OF BASE JOINT

The design of the base joint includes the determination of the E.D. and PT steel areas, probable (maximum) base moment strength of the wall, contract length and confinement reinforcement at the wall toes, E.D. steel strains and stresses (including the determination of the unbonded length for the E.D. bars), and PT steel strains and stresses (including the determination of the PT stress losses).

REINFORCEMENT CROSSING BASE JOINT

The PT and E.D. steel areas crossing the base joint can be estimated using fundamental concepts of reinforced and prestressed concrete mechanics (equilibrium, compatibility/kinematics, and design material constitutive relationships). A key parameter selected by the designer is the “E.D. steel moment ratio,” κ_d which is defined as:

$$\kappa_d = \frac{M_{ws}}{M_{wp} + M_{wn}} \quad (3)$$

where, M_{ws} , M_{wp} , and M_{wn} are the contributions of the E.D. steel, PT steel, and factored design gravity axial force, respectively, to satisfy the design base moment, M_{wd} . The κ_d ratio is a relative measure of the resisting moments from the energy dissipating force provided by the E.D. steel reinforcement and the vertical restoring (i.e., self-centering) force provided by the PT steel reinforcement plus the gravity axial load in the wall. If κ_d is too small, the energy dissipation of the wall may be very small. Conversely, if κ_d is too large, the self-centering capability of the wall may not be sufficient to yield the tensile E.D. bars back in compression and close the gap at the base joint upon the removal of the lateral loads.

Based on the performance of the specimens tested as part of this project,² the κ_d value used in design should not exceed 0.80 (to ensure sufficient self-centering) and should not be less than 0.50 (to ensure sufficient energy dissipation). Specimens with κ_d values close to both of these limits were tested (see Table 1). Fig. 2 shows the relative energy dissipation ratio, β of the six specimens as a function of wall drift. Specimen HW4, with design $\kappa_d=0.50$ and actual $\kappa_d=0.54$, satisfied the minimum $\beta_{min}=0.125$ requirement prescribed by ACI ITG-5.1 with a small margin, leading to the recommended lower limit of $\kappa_d=0.50$ for design. It should be noted that Specimen HW4 was a perforated wall, which increased the shear deformations in the wall panels resulting in reduced energy dissipation.² While it may be possible to use a reduced value for the lower κ_d limit for solid hybrid walls, this was not investigated by this research.

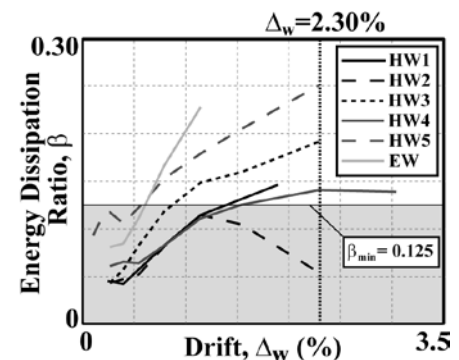


Fig. 2 Energy Dissipation Ratio

The recommended upper limit of $\kappa_d=0.80$ was selected based on the premature failure of Specimen HW5 (with design $\kappa_d=0.85$ and actual $\kappa_d=0.90$) prior to sustaining three loading cycles at the ACI ITG-5.1 validation-drift of $\Delta_w=2.30\%$. This specimen suffered from a loss of restoring and failed due to the uplift of the wall from the foundation (i.e., a gap formed along the entire base joint when the wall was unloaded to $\Delta_w=0\%$), which resulted in the subsequent out-of-plane displacements of the wall base and buckling of the E.D. bars in compression. Wall uplift and excessive out-of-plane displacements (or in-plane slip as was observed in Specimen EW) across the base joint can develop quickly and lead to failure with little warning. Fig. 3(a) shows the measured base shear force, V_b versus wall drift, Δ_w behavior of Specimen HW5 where the loss of restoring force can be seen by the unloading curves that do not return through the origin. Figs. 3(b) and 3(c) show the observed out-of-plane displacements and buckling of the E.D. bars at the base joint of the wall. The goal of the recommended upper limit on κ_d is to prevent this type of behavior.

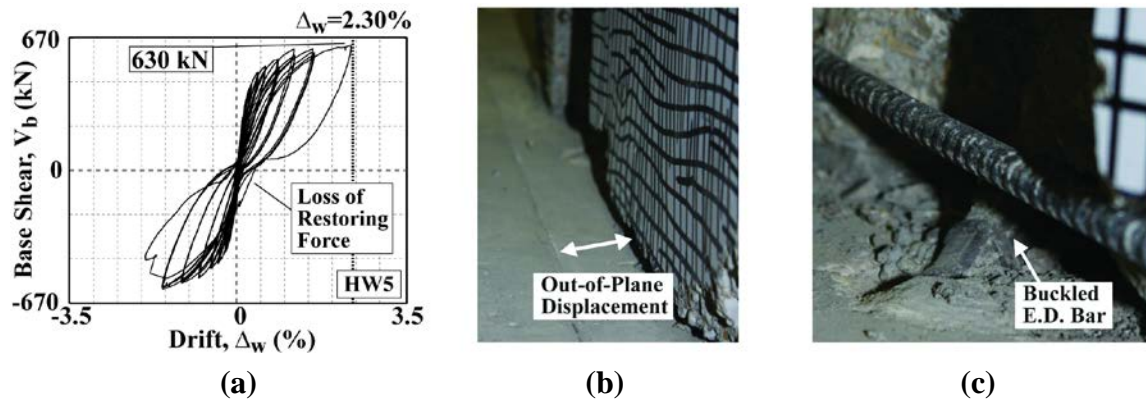


Fig. 3 Performance of Specimen HW5: (a) V_b - Δ_w Behavior; (b) Out-of-Plane Displacement; (c) Buckling of E.D. Bar

CONFINEMENT REINFORCEMENT AT WALL TOES

Confinement reinforcement is required at the ends of the base panel to prevent premature crushing and failure of the core (i.e., inner) concrete prior to the maximum-level drift, Δ_{wm} . The confinement steel ratio, hoop layout, and hoop spacing can be designed according to Sections 5.6.3.5 through 5.6.3.9 in ACI ITG-5.2. Based on the extent of the cover concrete spalling in the test specimens, the confined concrete region at the wall toes should extend vertically over a height of the base panel not less than the plastic hinge

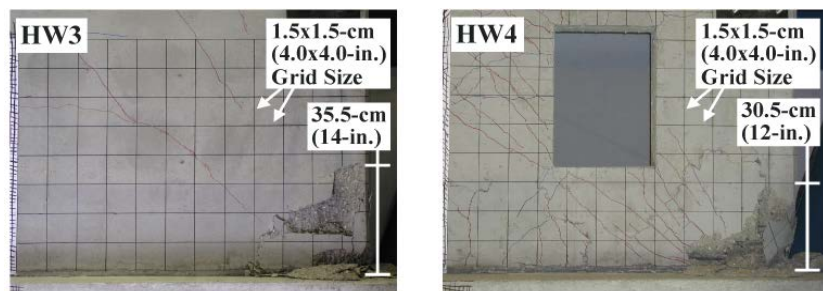


Fig. 4 North Toe at Base of Specimens HW3 and HW4

height, defined as $h_p=0.06H_w$ per ACI ITG-5.2. Fig. 4 shows the north toe at the base of Specimens HW3 and HW4 [where $h_p=33\text{-cm}$ (13-in.)] at the conclusion of each test. The observed extent of vertical cover spalling in Specimens HW3 and HW4 was approximately 35.5-cm (14-in.) and 30.5-cm (12-in.), respectively, supporting the design recommendation. Horizontally, the confined region should extend from each end of the base panel over a distance not less than $0.95c_m$ and not less than 30.5-cm (12-in.), as required by ACI ITG-5.2, where c_m =neutral axis length (i.e., contract length) at the wall base when Δ_{wm} is reached.

The design and detailing of the wall toes should also satisfy the applicable requirements for special boundary regions in Section 21.9.6.4 of ACI 318-11 as well as the bar spacing and concrete cover requirements in ACI 318-11. The height of the first confinement hoop from the base of the wall is critical to the performance of the confined concrete. The first hoop should be placed at a distance from the bottom of the base panel no greater than the minimum concrete cover required by ACI 318-11. This recommendation was not satisfied in Specimen HW1 (see Table 1), resulting in premature confined concrete crushing as show in Fig. 5(a).

Additionally, the length-to-width aspect ratio (measured center-to-center of bar) for rectangular hoops should not exceed 2.50. This requirement is slightly more conservative than but similar to past seismic design code specifications for boundary region confinement (e.g., see Section 1921.6.6.6 of the Uniform Building Code⁹), which have since been removed from the

current code requirements in the U.S. As observed from the performance of Specimen HW3 [see Fig. 5(a)], a large length-to-width ratio for the hoops can cause the bowing of the longer hoop legs in the out-of-plane direction, reducing the confinement effectiveness. Further,

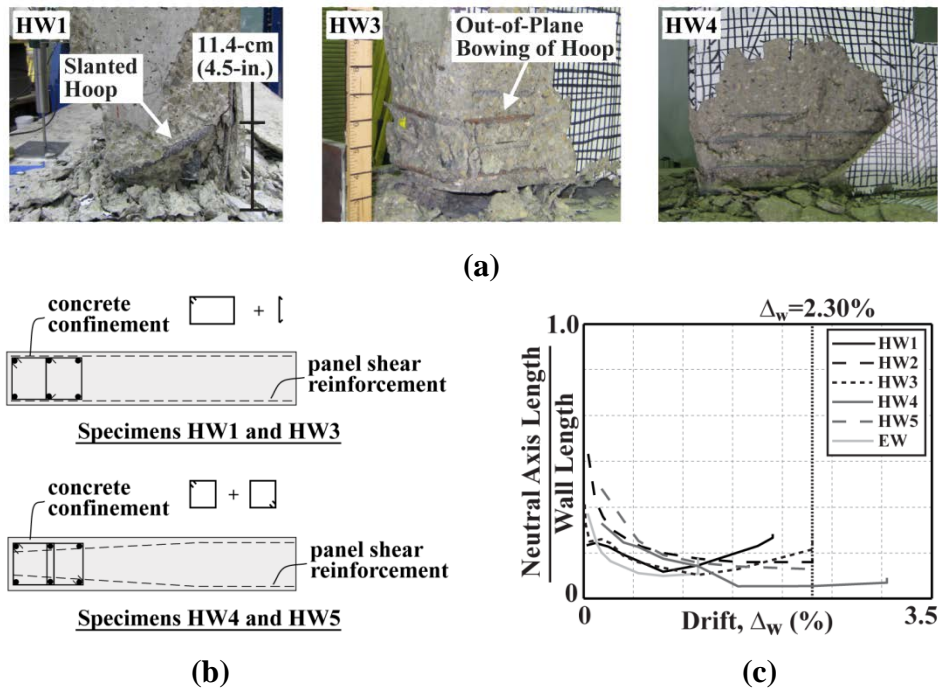


Fig. 5 Performance and Detailing of Confined Concrete Region: (a) Specimens HW1, HW3, and HW4; (b) Improved Hoop Detailing in Specimens HW4 and HW5; (c) Normalized Neutral Axis Length

intermediate crossties were ineffective in preventing the bowing of the longer hoop legs, since in typical construction the crossties do not directly engage the hoop steel (rather, the crossties engage the vertical reinforcement within the hoops). For comparison, Specimens HW4 and HW5 followed all of the above recommendations, resulting in excellent behavior of the confined concrete at the wall toes.² The performance of Specimen HW4 can be seen in Fig. 5(a) while the confinement detailing differences between the specimens is depicted in Fig. 5(b).

The confined concrete region performance is further demonstrated in Fig. 5(c), which plots the measured neutral axis length across the base-panel-to-foundation joint at the south end of the walls. During the small displacements of each wall, the neutral axis length went through a rapid decrease associated with gap opening at the base. As each wall was displaced further, the neutral axis length continued to decrease but at a much slower pace. Once deterioration of the concrete at the wall toes initiated, the neutral axis length began to elongate to satisfy equilibrium with the reduced concrete stresses. This effect is particularly evident during the final drift series for Specimens HW1 and HW3. For comparison, the neutral axis of Specimens HW4 and HW5 remained stable over a much larger drift range, as the elongation of the neutral axis length was not observed in Specimen HW5 and was evident in Specimen HW4 only after achieving the maximum-level drift, Δ_{wm} . The better performance of the confined concrete region in these specimens was due to the confinement steel detailing improvements shown in Fig. 5(b).

E.D. BAR STRAINS AND UNBONDED LENGTH

The seismic design of a hybrid precast wall requires the estimation of the E.D. bar strains. The elongations of the E.D. bars can be found by assuming that the wall displaces like a rigid body rotating through gap opening at the base joint.¹ The strain in each bar can then be calculated by dividing the bar elongation with the total unbonded length, which is taken as the sum of the wrapped length and an additional length of “debonding” that is expected to develop during the reversed-cyclic lateral displacements of the structure (estimated as the coefficient, α_s times the bar diameter per ACI ITG-5.2). The coefficient used to estimate this additional debonded length can be assumed as $\alpha_s=0$ and $\alpha_s=2.0$ at Δ_{wd} and Δ_{wm} , respectively. Concrete cores were taken through the thickness of the base panel around the end of the wrapped length of the E.D. bars in two of the specimens tested as part of this project, supporting the use of $\alpha_s=2.0$ at Δ_{wm} . The unbonded length (see Fig. 6) should be designed such that the maximum strains of the E.D. bars at Δ_{wm} are greater than $0.5\varepsilon_{su}$ to ensure sufficient energy dissipation but do not exceed $0.85\varepsilon_{su}$ to prevent low-cycle fatigue fracture, where ε_{su} is the monotonic strain capacity of the E.D. steel at peak strength. Strain limits ranging from $0.5\varepsilon_{su}$ to $0.85\varepsilon_{su}$ were used in the design of the test specimens (Table 1), with adequate energy dissipation and no bar fracture observed during the experiments. The

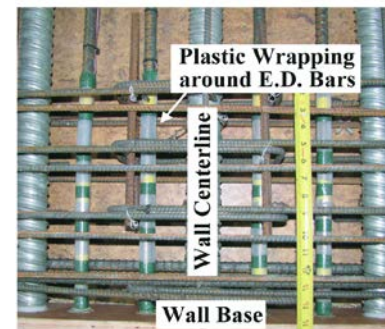
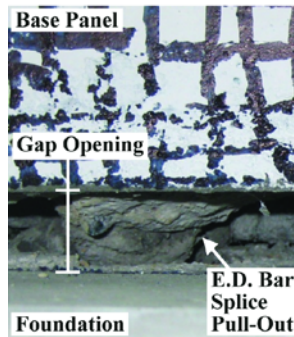


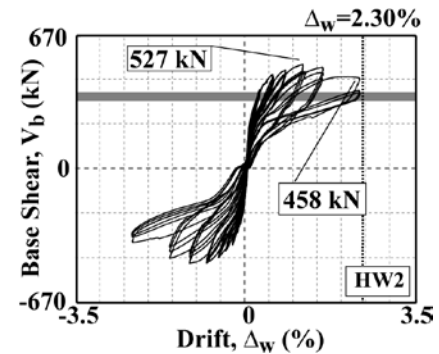
Fig. 6 E.D. Bar Wrapped Length in Specimen HW3

wrapped length can be located in either the bottom of the base panel or the top of the foundation; in either configuration, the E.D. bars should also be isolated from the grout through the thickness of the grout pad at the base joint (i.e., wrapped length should include the grout pad).

Sufficient development length should be provided at both ends of the wrapped region of the E.D. bars. Due to the large cyclic steel strains expected through Δ_{wm} , Type II mechanical splices specified in Section 21.1.6 of ACI 318-11 and permitted by Section 5.4.2 of ACI ITG-5.2 should not be used for the E.D. bars in hybrid precast walls in seismic regions unless the splices have been tested and validated under cyclic



(a)



(b)

Fig. 7 Performance of Specimen HW2:
(a) E.D. Bar Splice Pullout; (b) V_b - Δ_w Behavior

loading up to a steel strain of at least $0.85\epsilon_{su}$. In Specimen HW2, pullout of the E.D. bars [see Fig. 7(a)] from the foundation occurred due to failure of the grout within Type II splice connections prior to Δ_{wm} . The pullout caused the E.D. bar elongations and strains to be smaller than designed, resulting in smaller lateral strength and energy dissipation of the wall (see Fig. 2). Fig. 7(b) shows the measured V_b - Δ_w behavior with the gray shaded band indicating the calculated strength of the wall ignoring the E.D. bars. Comparing this range with the measured behavior, Specimen HW2 was essentially behaving as a fully post-tensioned wall by the end of the test due to the failure of the E.D. bar splice connections.

While the splices used in Specimen HW2 satisfied all ACI 318-11 and AC33¹⁰ performance requirements for Type II mechanical connectors and the grout used inside the splices satisfied the splice manufacturer's specifications, the E.D. bars were subjected to greater strains and over a significantly larger number of cycles than required to classify a Type II connection per ACI 318-11 and AC133, resulting in pullout of the bars. Therefore, it is recommended that in validating Type II connectors for use in E.D. bar splices, the bars be first subjected to 20 cycles of loading through $+0.95\epsilon_{sy}$ and $-0.5\epsilon_{sy}$, where ϵ_{sy} =yield strain of the steel, as required by AC133. Beyond this point, 6 cycles should be applied at each load increment, with the compression strain amplitude kept constant at $-0.5\epsilon_{sy}$ and the tension strain amplitude increased to a value not less than $5/4$ times and not more than $3/2$ times the strain amplitude from the previous load increment. Testing should continue until the tension strain amplitude reaches or exceeds $+0.85\epsilon_{su}$ over 6 cycles.

In lieu of Type II mechanical splices, the full development length of the E.D. bars can be cast or grouted (during the construction process) into the base panel and the foundation. This

connection technique was successfully used in this project, with no pullout of the bars from the concrete.²

FLEXURAL DESIGN OF UPPER JOINTS

The E.D. bars crossing the base joint do not continue into the upper panel-to-panel joints, resulting in a significant reduction in the lateral strength of the wall at these locations. The philosophy behind the flexural design of the upper joints is to prevent significant gap opening and nonlinear behavior of the material through the maximum-level drift, Δ_{wm} . Thus, the design of the upper panel-to-panel joints is conducted for the maximum joint moment demands corresponding to the probable base moment strength, M_{wm} of the wall. To prevent significant gap opening at the upper joints, mild steel reinforcement should be designed at the panel ends, as shown in Fig. 1. The design of this reinforcement is based on the principles of equilibrium, linear material models, and a linear strain distribution (i.e., plane sections remain plane). The design requires that the tension steel strain be limited to ϵ_{sy} (to limit gap opening) and the maximum concrete compressive stress be limited to $0.5f'_c$ (to keep the concrete linear elastic), where ϵ_{sy} =yield strain of the mild steel, and f'_c =compression strength of the unconfined panel concrete. These material limits were used in the design of the wall specimens tested as part of this project, with no undesirable behavior developing in the upper joints.² To prevent strain concentrations in the steel, a short prescribed length of the bars [approximately 10 to 15-cm (4 to 6-in.)] should be unbonded at each joint.

SHEAR DESIGN ACROSS JOINTS

To prevent significant horizontal slip of the wall during loading up to Δ_{wm} , the shear friction capacity at the horizontal joints should be greater than the shear force demand. The joint shear forces should be calculated from the maximum base shear force, V_{wm} corresponding to the probable base moment strength, M_{wm} of the wall at Δ_{wm} . The nominal shear friction strength at the base joint can be calculated as the friction coefficient, $\mu_{ss}=0.5$ multiplied by the compressive force in the contact region at the wall toe. For the upper joints, μ_{ss} is taken as 0.6 and the shear friction strength from the axial force due to the PT steel and the gravity load is combined with the shear friction strength from the yielding of the mild steel bars crossing the joint at both ends (similar to the shear friction design method in Section 11.6 of ACI 318-11). As recommended in Section 5.5.3 of ACI ITG-5.2, the larger μ_{ss} for the upper joints as compared with the base joint is because deterioration to the grout and concrete at the base joint could lead to reduced slip strength.

The specimens tested as part of this project were designed using the above approach, with the measured slip at the centerline along the base joint shown in Fig. 8(a). No appreciable slip was measured or observed in the upper joints of the test specimens. For walls that satisfied the axial restoring force requirement described later in this paper (Specimens HW1, HW2,

HW3, and HW4), only a small amount of shear slip occurred along the base joint. In some instances, base slip of up to 0.38-cm (0.15-in.) was measured, exceeding the allowable limit of 0.15-cm (0.06-in.) per Section 7.1.4(3) of ACI ITG-5.1. However, this slip did not result in any undesirable behavior of the walls. Therefore, the shear slip limit in ACI ITG-5.1 can be increased to 0.38-cm (0.15-in.)

without affecting the wall performance. Specimens HW5 and EW did not satisfy the restoring force requirement, resulting in excessive slip at the base. Under load reversal with increasing slip, the concrete around the E.D. bars in Specimen EW began to deteriorate due to the shear force transfer from the bars to the surrounding concrete, ultimately causing failure through localized splitting of the base panel around the bars [see Fig. 8(b)].

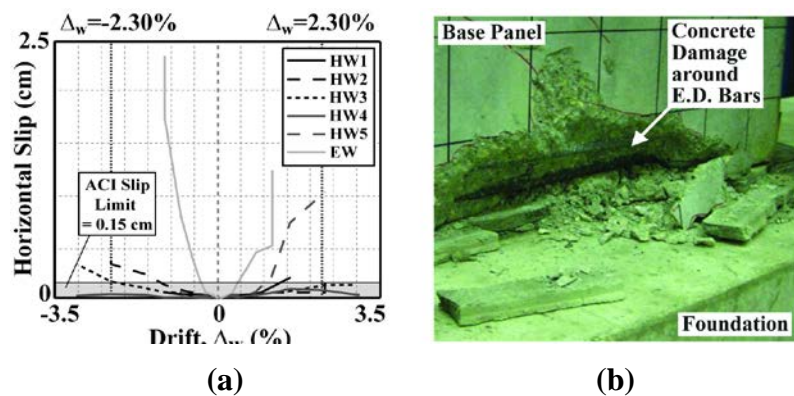


Fig. 8 Horizontal Slip Along Base Joint: (a) Measured Slip; (b) Base Panel Damage in Specimen EW

WALL PANEL REINFORCEMENT

The wall panel steel reinforcement that is not continued across the horizontal joints includes shear reinforcement, edge reinforcement, and reinforcement to control temperature and shrinkage cracks as

well as to support lifting inserts. Based on the performance of the test specimens, the base panel of a hybrid precast wall is expected to develop diagonal cracking; and thus, distributed vertical and horizontal reinforcement should be designed following the applicable requirements in Sections 21.9.2 and 21.9.4 of ACI 318-11. As shown for Specimens HW3 and HW4 in Fig. 9, the specimens that satisfied these requirements had well distributed hairline cracking in the base panel (note that the cracks visible in the photographs were highlighted with markers during the test for enhanced viewing). The upper panels of the solid walls developed no cracking; and thus, the distributed reinforcement in these panels can be reduced following the requirements in Section 16.4.2 of ACI 318-11. In perforated walls, the reinforcement in both the base and the upper panels should be designed following the Design Procedure Document,¹ which uses a finite element analysis of the wall through Δ_{wm} .



Fig. 9 Base Panel of Specimens HW3 and HW4

Section 21.9.6.4(e) of ACI 318-11 should be satisfied for the development of the base panel horizontal reinforcement in the confined boundary regions at the wall toes. The horizontal bars in Specimens HW1, HW2, and HW3 were not developed inside the boundary regions [see Fig. 5(b)], reducing the effectiveness of these bars and causing increased spalling and delamination of the cover concrete at the base [see Fig. 5(c)]. In addition, reinforcement should be placed around the entire perimeter of each wall panel using mild steel bars placed parallel to each panel edge. As required by Section 4.4.10 of ACI ITG-5.2, the mild steel reinforcement along the bottom edge of the base panel should provide a nominal tensile strength of not less than 87.6-kN per horizontal meter (6000-lbs per horizontal foot) along the length of the panel. The bottom edge bars should be anchored using a standard 90° hook at the panel corners with sufficient development length from the critical location at the neutral axis (i.e., at a distance c_m from each end of the wall). The objective of this reinforcement is to control concrete cracking initiating from the bottom of the base panel near the tip of the gap; and thus, the bars should be placed as close to the bottom of the panel as practically possible, while also satisfying the ACI 318-11 concrete cover and spacing requirements. The bottom edge reinforcement in the walls tested as part of this project was designed using this approach. Strain gauges placed on the bars indicated strains reaching approximately $0.85\varepsilon_{sy}$ at Δ_{wm} , supporting the design requirement.

WALL RESTORING FORCE

Hybrid precast walls must maintain an adequate amount of restoring force (i.e., self-centering capability) to ensure that the gap at the base joint is fully closed upon removal of the lateral load after tensile yielding of the E.D. bars. This restoring force, which is comprised of the gravity axial force and the total PT force including losses¹ at Δ_{wm} ,

should be greater than $A_s(f_{sm}+f_{sy})$, where A_s =total area of the E.D. steel, f_{sm} =E.D. steel stress at Δ_{wm} , and f_{sy} =yield strength of the E.D. steel. This is demonstrated in Fig. 10(a), which shows an idealized stress-strain relationship for the E.D. steel. As the wall is displaced from the initial position (close to Point A), the E.D. bars yield in tension (Point B) and reach the maximum strain, ε_{sm} (Point C) at Δ_{wm} . Upon unloading of the wall, the restoring force must be able to yield the tensile E.D. bars back in compression (Point D) and return the bars to essentially zero strain (Point E), resulting in a total force reversal of approximately

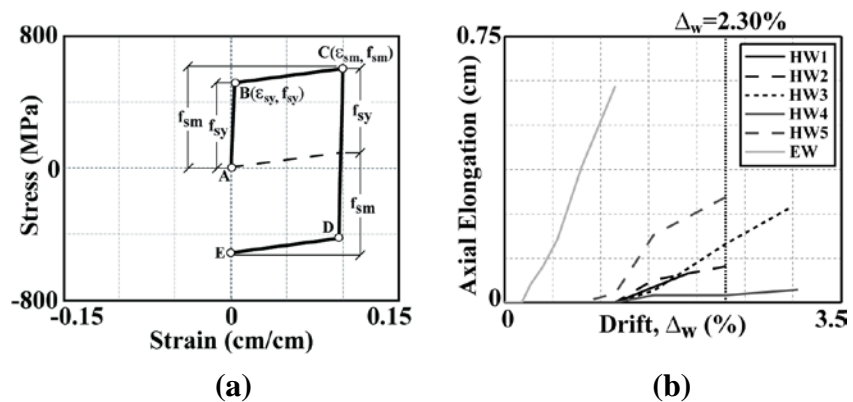


Fig. 10 Restoring Force: (a) Idealized E.D. Steel Stress-Strain Relationship; (b) Residual Wall Uplift

$A_s(f_{sm}+f_{sy})$ such that no significant plastic tensile strains accumulate in the steel. The elastic unloading force provided by the E.D. steel is ignored.

This requirement is more demanding than that given in Section 5.3.1 of ACI ITG-5.2. The restoring force in Specimen HW5 was close to the ACI ITG-5.2 limit, but was not sufficient to overcome $A_s(f_{sm}+f_{sy})$. Fig. 10(b) shows the residual axial elongation (upwards positive) measured at the centerline of each wall at the same elevation as the applied lateral load upon unloading to $\Delta_w=0\%$ from the 3rd cycle in each drift series. The accumulation of this residual axial elongation represents a reduction or loss of the axial restoring force in the system. Specimens HW1, HW2, HW3, and HW4 satisfied the restoring force requirement of this paper. The axial elongation in these walls did not start to accumulate until the $\Delta_w=\pm 1.55\%$ drift series, which coincided with the initiation of PT stress losses. This small amount of uplift did not affect the performance of the wall in any undesirable way. However, in Specimen HW5, the residual axial elongation started to accumulate earlier (during the $\Delta_w=\pm 1.15\%$ drift cycles) and the maximum residual elongation at $\Delta_w=2.30\%$ was almost twice as large. Over successive loading/unloading cycles with increasing wall drift, the residual tensile deformations in the E.D. bars resulted in the complete uplift of the wall, overcoming the downward restoring force. The subsequent failure of the structure occurred rapidly (and before three cycles at Δ_{wm} were sustained) due to out-of-plane displacements of the wall base during unloading and buckling of the E.D. bars (Fig. 3). The deterioration in Specimen EW, which had no PT force (and thus, an even smaller amount of restoring), began earlier (during the $\Delta_w=\pm 0.27\%$ cycles) leading to excessive in-plane slip at the base joint and splitting of the base panel.

SUMMARY AND CONCLUSIONS

This paper summarizes key aspects of a Design Procedure Document¹ for special unbonded post-tensioned hybrid precast shear walls in seismic regions. The proposed design guidelines were developed and validated using the measured behaviors from six 0.4-scale multi-panel test specimens (four solid and two perforated walls) subjected to service-level gravity loads combined with reversed-cyclic lateral loading. Ultimately, these requirements are aimed to allow practicing engineers and precast producers to design ACI-compliant special hybrid precast shear walls with predictable, reliable, and improved seismic performance.

ACKNOWLEDGEMENTS

This research was funded by the Charles Pankow Foundation and the Precast/Prestressed Concrete Institute (PCI). Additional technical and financial support was provided by the High Concrete Group, LLC, the Consulting Engineers Group, Inc., and the University of Notre Dame. The authors would like to acknowledge the support of the PCI Research and Development Committee as well as the members of the Project Advisory Panel, who include

Walt Korkosz (chair) of the Consulting Engineers Group, Inc., Ken Baur of the High Concrete Group, LLC, Neil Hawkins of the University of Illinois at Urbana-Champaign, S.K. Ghosh of S.K. Ghosh Associates, Inc., and Dave Dieter of Mid-State Precast, LP. Additionally, the authors thank Prof. Michael McGinnis and his student, Michael Lisk from the University of Texas at Tyler for monitoring the response of the wall test specimens using three dimensional digital image correlation (3D-DIC). Material donations were provided by Jenny Bass of Essve Tech Inc., Randy Ernest of Prestress Supply Inc., Randy Draginis and Norris Hayes of Hayes Industries, Ltd., Rod Fuss of Ambassador Steel Corporation, Chris Lagaden of Ecco Manufacturing, Stan Landry of Enerpac Precision SURE-LOCK, Richard Lutz of Summit Engineered Products, Shane Whitacre of Dayton Superior Corporation, and Steve Yoshida of Sumiden Wire Products Corporation. The authors thank these individuals, institutions, and companies for supporting the project. The opinions, findings, conclusions, and/or recommendations expressed in this paper are those of the authors and do not necessarily represent the views of the individuals and organizations acknowledged.

REFERENCES

1. Smith, B., Kurama, Y., "Seismic Design Guidelines for Special Hybrid Precast Concrete Shear Walls," Univ. of Notre Dame, Res. Rep. No. NDSE-2012-02, Notre Dame, IN, June 2012.
2. Smith, B., Kurama, Y., McGinnis, M., "Hybrid Precast Wall Systems for Seismic Regions," Univ. of Notre Dame, Res. Rep. No. NDSE-2012-01, Notre Dame, IN, June 2012.
3. Smith, B., Kurama, Y., McGinnis, M., "Design and Measured Behavior of a Hybrid Precast Concrete Wall Specimen for Seismic Regions," *J. Struct. Eng.*, 137(10), 2011, 1052-1062.
4. Smith, B., Kurama, Y., McGinnis, M., "Design and Measured Behavior of a Perforated Hybrid Precast Concrete Shear Wall for Seismic Regions," *PCI Annual Convention and Exhibition*, Salt Lake City, UT, 2011.
5. ACI 318, "Building Code Requirements for Structural Concrete (ACI 318-11) and Commentary," ACI Committee 318, Farmington Hills, MI, 2011.
6. ACI ITG-5.1, "Acceptance Criteria for Special Unbonded Post-Tensioned Precast Structural Walls Based on Validation Testing and Commentary," ACI Innovation Task Group 5, Farmington Hills, MI, 2007.
7. ACI ITG-5.2, "Requirements for Design of a Special Unbonded Post-Tensioned Precast Shear Wall Satisfying ACI ITG-5.1 and Commentary," ACI Innovation Task Group 5, Farmington Hills, MI, 2009.
8. ASCE, "Minimum Design Loads for Buildings and Other Structures," ASCE/SEI 7-10, 2010.
9. ICBO, "Uniform Building Code, Volume 2: Structural Engineering Design Provisions," International Conference of Building Officials, 1997.
10. ICC, "AC133: Acceptance Criteria for Mechanical Connector Systems for Steel Reinforcing Bars," ICC Evaluation Services, 2010.